Pergamon

Int. J. Multiphase Flow Vol. 24, No. 1, pp. 35–54, 1998

Printed in Great Britain
PII: S0301-9322(97)00046-3
0301-9322/98 $19.00 + 0.00

EXPERIMENTAL INVESTIGATION OF A TURBULENT BUBBLY MIXING LAYER

V. ROIG, C. SUZANNE and L. MASBERNAT

Institut de Mécanique des Fluides, UMR CNRS 5502, Avenue du Professeur Camille Soula, 31400 Toulouse, France

(Received 8 May 1994; in revised form 12 June 1997)

Abstract—An experimental investigation of a turbulent air–water bubbly flow in a plane vertical mixing layer is presented. An important characteristic of this bubbly flow is that the slip velocity is of the same order of magnitude as the liquid velocity. For various inlet conditions of liquid velocity and void fraction, the distributions of velocity, turbulence intensity and void fraction were measured. The mean velocity fields in both phases present self-similar evolutions that preserve the main characteristics of single-phase mixing layer. The spreading rate of the mixing layer is found to be significantly greater in bubbly flow than in single-phase flow. Moreover, the global structure of the flow proved to be sensitive to void fraction contrast at the inlet. The void fraction distributions exhibit a pronounced peak in the wake of the splitter plate. This peak decreases in intensity and is displaced significantly in the lateral direction. The turbulence intensity is also greater in bubbly mixing layers: it is shown that this effect is related to the bubble drift velocity. A heuristic model for the separation of bubble and shear-induced velocity fluctuations is presented and discussed. Finally, it is observed that the RMS velocity of the gas phase results from combined effects of turbulent dispersion and self-induced fluctuating motions of the bubbles. © 1997 Elsevier Science Ltd

Key Words: bubbly flow, mixing layer, turbulence, bubble-induced "pseudo-turbulence", local measurements

1. INTRODUCTION

During the last decade, a great effort has been undertaken for the development of multidimensional numerical models for the prediction of two-phase flows (Drew and Wallis 1994; Bel Fdhila and Simonin 1992). However, the predictions of velocities and phase distributions in dispersed flows in complex geometries have demonstrated the limits of these models (Lance and Lopez de Bertodano 1994). These limitations are mainly due to the inadequacy of the closure laws expressing the interfacial momentum transfer and the turbulence of each phase. Owing to the complexity and the multiplicity of the physical phenomenon to be modelled, it is necessary to carry on theoretical and experimental analyses of basic two-phase flows.

Some basic experiments have already been completed to clarify the structure of turbulent bubbly flows. Serizawa *et al.* (1975), Wang *et al.* (1987, 1990) studied bubbly flows in pipe in which the mean features of turbulence and void fraction distributions are displayed close to the solid wall. Drew and Lahey (1982) demonstrated that the correct modelling of the turbulent Reynolds stress of the continuous phase is crucial for the prediction of the void distribution in pipes. More recently, Bel Fdhila *et al.* (1990) explored a bubbly flow through a sudden expansion: they gave evidence of the major effect of the nonlinear turbulent momentum transfer terms on the void migration. These studies clearly emphasize the dominant role of the turbulence behaviour upon the void distribution.

Another peculiarity of turbulent bubbly flow is that the mean bubble diameter is usually greater than the Kolmogorov length scale, in contrast to particulate flows. It is thus expected that the relative motion of the bubbles modifies the turbulent field of the continuous phase. This is confirmed in several experiments in which the drift velocity is comparable to the liquid velocity (Theofanous and Sullivan 1982; Lance and Bataille 1991; Lance *et al.* 1991). Indeed, an important modification of the single-phase turbulence may be observed, even at low void fraction. Lance

and Bataille investigated a uniform bubbly flow in a turbulence field generated through a grid. They showed that, at low void fraction, the measured turbulent kinetic energy of the liquid may be approximated by the sum of the turbulent kinetic energy in the absence of bubbles (a "shear-induced" turbulence) and a kinetic energy due to the action of bubbles undergoing helicoidal paths in an ideal fluid (the "pseudo-turbulence"). This pseudo-turbulence has been theoretically put into light by Van Wijngaarden (1976) and confirmed later by Drew and Wallis (1994) from inviscid fluid analysis. The motion of bubbles generates random velocity fluctuations due to the inhomogeneities of the potential flow around the bubbles in their random trajectories. The bubble-induced fluctuations also consist of small scale eddies generated by vortex shedding in the bubble wakes as well as by bubble interface deformation. In several bubbly flow experiments, viscous dissipation was also found to be controlled mainly by bubble-induced effects (Wang *et al.* 1990; Lance and Bataille 1991). Lance and Bataille found that, for negligible accelerations of the relative movement in large scale motion, the dissipation rate in the wakes of the bubbles is balanced by the power of the drag force exerted by the bubbles on the fluid. It thus appeared that in bubbly flows where the entrainment of the bubbles by large eddies was negligible, pseudo-turbulence induced by added mass effects in helicoidal movements and fluid motions in bubble wakes could be separated from an energetic point of view. However, an important issue concerns the role of the bubble-induced turbulence in the turbulent momentum transport, which has not yet been clarified (Lance and Lopez de Bertodano 1994).

The present study is devoted to an experimental investigation of a turbulent bubbly flow in a plane vertical mixing layer. The flow conditions are characterised by a ratio of bubble diameter to turbulence microscale close to unity, a ratio of slip velocity to liquid velocity close to unity, and a void fraction less than 3%. The mean bubble diameter was about 2 mm and the liquid velocity did not exceed 1 m/s. Because of the high turbulence level and strong shear stress, the turbulent bubbly shear layer remains a fundamental case to study. Existing measurements in bubbly jets (Sun and Faeth 1986) where done for higher liquid velocities, thus masking bubble-induced turbulence effects. In our flow conditions, the velocity of the liquid phase being comparable to the slip velocity, the contribution of the bubble drift may be significant compared to the contribution of the shear stress. The mixing layer allows investigation of the role of both shear-induced and bubble-induced turbulence. Moreover, the present experimental investigation provides new insights into interfacial momentum transfer as well as bubble dispersion mechanisms which are not clearly understood in inhomogeneous flows.

Local measurements presented in this paper include mean and fluctuating velocities of both phases. The U-components of the velocities of each phase in the streamwise direction were measured. These measurements provide some interesting preliminary information about the structure of the velocity field in nearly parallel 2D flow. Void fraction and bubbles sizes were also measured. The results were obtained for various inlet conditions of liquid velocity and void fraction.

The experimental facility and the measuring methods are, respectively, described in sections 2 and 3. Test conditions are presented in section 4, experimental results are reported and discussed in sections 5–9. It will be shown that the mean velocity of both phases presents a self-similar evolution. The turbulence in the liquid is enhanced by the presence of the bubbles. A separation of bubble and shear-induced turbulence shows that experimental results, obtained in bubbly grid-generated turbulence by Lance and Bataille (1991) and concerning bubble-induced turbulence, still hold in the low void fraction mixing layer. Finally, the ratio of gas and liquid velocity fluctuations is found nearly constant and compared to Tchen's theory.

2. EXPERIMENTAL FACILITY

In order to achieve the investigation of bubbly flow in a mixing layer, an experimental facility described in detail in Roig (1993) has been built. A schematic diagram of this facility is given in figure 1. The experimental facility consists of a vertical square channel of 2 m height and 0.4×0.4 m^2 cross-sectional area, where the mixing layers develop from bottom to top. The channel is operated at normal temperature and pressure conditions. The channel is supplied at bottom by

an inlet feeder consisting of a stagnation chamber (3 m^3) and a convergent section (14:1 ratio, 0.9 m height) both divided into two parts by a vertical splitter plate of 2 mm thickness with a cusped trailing edge. Each part is supplied independently by a bubbly flow of given air and water rates. The liquid velocities at the inlet can be adjusted between 0 and 1 m/s and the void fraction can be up to 5%. The high contraction intake, the screening and the honeycomb section provide a uniform velocity profile at the entrance. The turbulence intensities outside the mixing layers were found to be less than 3% in single-phase flows.

Air bubbles are injected just before the convergent section: for each stream, the bubble injector is made up of three porous tubes horizontal and parallel to the splitter plate. Stainless steel sintered porous tubes with 23 mm external diameter and 60 cm effective injection length are used. The tubes are located at horizontal distances of 6, 18 and 30 cm from the splitter plate. Previous experiments show that the presence of the tubes does not affect the inlet conditions. Nevertheless, all the results that are reported, in two-phase runs as well as in single-phase runs, were obtained in the final set-up in the presence of the bubble injectors. Uniform void fraction profiles were obtained at the inlet section in the core region of the flow. However, near the splitter plate, at a distance of about one bubble diameter from the wall, there existed one or two peaks of void fraction due to the development of the boundary layers on each side of the plate. The ideal situation would have been to produce the mixing layer from two inlet flows with uniform velocity, turbulence and void fraction. Whatever, the inlet conditions were carefully explored and reported for each run (Roig 1993).

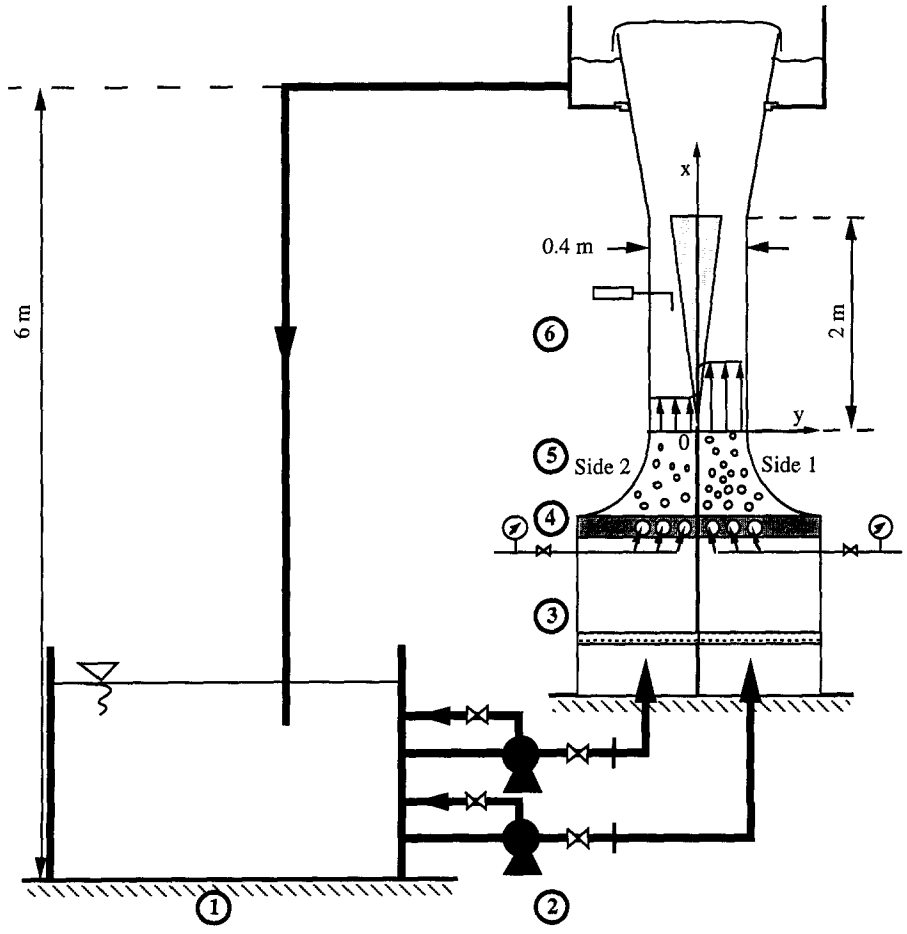

Figure 1. Schematic diagram of the test facility. 1: Water tank (10 m^3); 2: pumps; 3: screening section (3 m^3); 4: air feeding; 5: convergent section; 6: measuring section.

Water is collected in the upper reservoir, and gravity-fed into the lower reservoir. The test section is equipped with a traversing mechanism allowing the displacement of the measuring probes in the (x, y) vertical plane, where x and y denote the streamwise and transverse coordinates, respectively (see also figure 1). The origin of the Cartesian coordinates is located at the end of the trailing edge of the splitter plate.

Previous measurements using a laser Doppler velocimeter showed that the main characteristics of the flow field—mean velocity, turbulence intensity—in the absence of bubbles are constant along the z direction. In two-phase flows, visualisations of nearly two-dimensional large coherent structures confirmed that the mixing layer remains plane.

3. MEASUREMENT METHOD AND SIGNAL PROCESSING

For single-phase flows, both laser Doppler (LDA) and hot film anemometers (HFA) were used for the velocity measurement method and the flow structure to be qualified. In the bubbly flows, only the HFA was used due to the difficulty of obtaining a correct Doppler signal from LDA. The void fraction, bubble diameter and velocity were obtained from optical fibre probes (OFP). For numerical processing, the HFA and OFP probe signals were recorded on an HP1000 computer unit at a sampling frequency of 5 kHz. The frequency bandwidth more than spans the realm of significant energy content in the turbulence. Moreover, the sampling frequency allows us to define the signal of bubble passage with a sufficient number of samples.

3.1. *Measurements in the liquid phase*

The HFA was composed of a single cylindrical hot film probe, a constant temperature anemometer and a linearizer. The overheat ratio was kept constant and equal to 0.06. The linearized signal was fed into the HP1000 computer unit for numerical processing. The time of measurement necessary for the average to converge was about 2 min.

When the film is in the gas, the signal is no longer representative of the velocity: it is thus necessary to remove this part of the signal. The phase discrimination is based on a thresholding technique applied to the derivative of the signal. This derivative greatly magnifies the drop due to the bubble passage and allows an easy discrimination of the phases.

It is unfortunately not clear at the present moment whether or not the decreasing part of the rear peak clearly observed on the signal just after the passage of a bubble is a correct signature of the bubble drift. The overshot observed in air–water experiments should be related to wetting phenomenon, as put into light by Gherson and Lykoudis (1984) who did not observe trailing peaks in mercury with normal gravity conditions. On another side, those peaks have been observed in an LDA signal by Theofanous and Sullivan (1982) who suggested that the overshot signifies the slip velocity. In this work, we retained most of the peak contributions as representative of the local inhomogeneities of the flow around the pierced bubbles.

Errors on mean and RMS liquid velocity measurements are related to finite time average and phase discrimination. The mean velocity relative error due to finite time average has be estimated lower than 3% in single-phase and bubbly flows. In bubbly flows, an upper bound for the relative error of mean velocity measurement due to phase discrimination is 2%. But phase discrimination, that is retaining or not the trailing peak at the rear of the bubble passage as significant of liquid velocity, can change notably the estimation of the turbulent intensity. An estimation of this difference is given by processing a bubbly test signal such as to cut more or less the peaks at bubble passages. Removing entirely these parts of the signal would have induced a 15% decrease of the turbulent intensity.

3.2. *Measurements in the gas phase*

For void fraction measurements, a single RBI monofibre probe whose tip diameter was less than 50 μm was used. An indication of the presence of either phase on the OFP relies on the change of optical index between the two media. The conversion of the OFP signal into a numerical two-state signal consisted in a thresholding technique. Small tip diameter and sharp geometry of the OFP ensured correct piercing of the bubbles and reduced the response time. For monofibre probes, Cartellier (1990) showed that the duration of the signal rise due to plane interface piercing

Table 1. Inlet conditions of the different tests (at $x = -1$ cm). Experimental expansion parameters

Run	1–1	1–2	2–1	2–2	2–3	2–4
ϵ_{10} (%)	0.0	1.9	0.0	1.9	1.9	0.0
U_{L10} (m/s)	0.87	0.95	0.615	0.53	0.51	0.58
ϵ_{20} (%)	0.0	1.9	0.0	1.9	0.0	1.5
U_{L20} (m/s)	0.55	0.60	0.255	0.23	0.18	0.19
ΔU_{L0} (m/s)	0.32	0.35	0.36	0.3	0.33	0.39
U_{Lm0} (m/s)	0.71	0.775	0.435	0.38	0.345	0.385
$\lambda_0 = \Delta U_{L0}/2U_{Lm0}$	0.225	0.226	0.414	0.395	0.478	0.506
x_M (m)	1.0	0.60	1.4	0.50	1.0	0.40
Measurement in gas phase	—	Not made	—	Yes	Yes	Yes
$\frac{dB_L}{dx}$	6.6×10^{-2}	0.15	7.4×10^{-2}	0.188	0.139	0.205
σ_L	30	13	24	11	13	14
σ_G	—	Not made	—	9	12	14

was less than 0.3 ms for interface velocity higher than 0.3 m/s. In our bubbly flows, the response time was always smaller than the sampling time. The phase discrimination thus induced less than 4% errors on the local measurement of mean void fraction ϵ.

Few authors have measured the bubble velocity and bubble fluctuations in turbulent flows. Among them, Herringe and Davis (1976) and Van der Welle (1985) have obtained the mean bubble velocity by cross-correlating the signals from two different probes, whereas the determination of the bubble velocity fluctuations was reported by Serizawa *et al.* (1975) and Sun and Faeth (1986). The OFP measuring method developed in this work allows us to determine the mean and fluctuating velocities as well as a characteristic bubble size. It has some common features with the method of Serizawa *et al.* (1975). Whereas they used an analogical signal processing, we chose a numerical multichannel analysis of the binary signals obtained from a double monofibre optical probe.

The velocity of the bubble is determined by the time lag $\Delta\tau$ displayed when a bubble crosses the two probes and a knowledge of the distance between the probes, which is equal to 3.8 mm. The chord length of a bubble crossing is then calculated from the residence time on the first probe, Δt.

Selective criteria are applied in order to avoid taking into account erroneous situations when two different bubbles cross the probes (see Serizawa *et al.* 1975). In a first stage, we decide if the current time lag $\Delta\tau$ is plausible or not by comparison with the most probable time lag $\Delta\tau_m$ estimated at each point from the cross-correlation function. Then, undetermined situations can occur, because it often happens that two consecutive bubble impacts on one of the sensors respect a correct time lag with one (or more) impacts on the other sensor. An additional criterion is thus introduced to validate measurement. It is based on the adequacy of the numbers of bubbles that have crossed, respectively, each probe in the required time lag. Signals of each probe are retained to calculate both velocity and size only when this criterion is satisfied.

The method of measurement was checked in a still water tank where bubbles were injected. A high speed video camera allowed us to validate the bubble mean velocity and mean size measurements. The relative errors in measurements of bubble mean velocity and mean size are both less than 5%.

In the mixing layer, the typical number of validated events necessary for the statistical averaging of the gas RMS velocity to converge was about 1500. The ratio between the number of retained events and the number of bubbles seen by one of the probes was about 70%.

4. TEST CONDITIONS

Local measurements were performed for six different inlet flow conditions, in several test sections: one was located upstream from the trailing edge of the splitter plate, at $x = -1$ cm, and the others were located downstream, up to a maximum height x_M depending on the flow development. The value of x_M is given in table 1. The choice of the maximum height section was

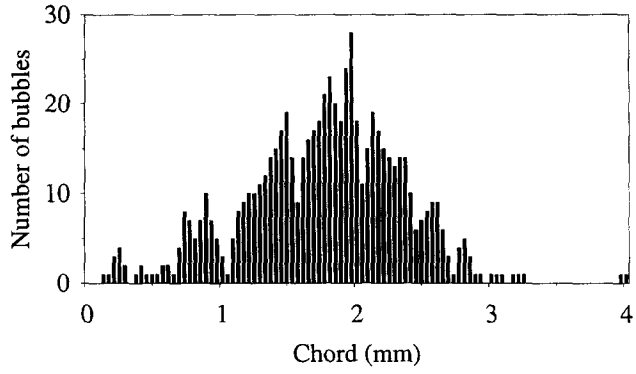

Figure 2. Typical bubble chord histogram.

such that no interaction between the mixing layer and the walls was observed in the measuring area.

For each run, the values of both liquid velocity and void fraction in the core region of both layers before mixing are indicated in table 1. The conventional notations are reported in figure 1. Subscripts L or G will denote liquid phase or gas phase. Subscripts 1 and 2 correspond to each core region at $y > 0$ and $y < 0$, respectively. Subscript 0 denotes inlet conditions.

The mixing layer is characterised by the liquid velocity ratio $\lambda = \Delta U_L / 2U_{Lm}$, where $\Delta U_L = U_{L1} - U_{L2}$ is the liquid velocity difference across the mixing zone and $U_{Lm} = \frac{1}{2}(U_{L1} + U_{L2})$ is its mean liquid velocity. The Reynolds number, defined for mixing layers with the longitudinal coordinate x as $\mathrm{Re} = \Delta U_L x / \nu_L$, varies within the range [1.9×10^4 to 4.4×10^5] between the first and the last measuring sections. These Reynolds numbers clearly indicate that the flows are turbulent.

The runs 1–1 and 2–1 are single-phase mixing layers with two different liquid velocity ratios λ, but nearly the same value of ΔU_L. These two runs will allow comparison with two-phase flows developing from similar inlet conditions of liquid velocity. Bubbly mixing layers 1–2 and 2–2 have inlet velocities quite identical to the velocities of the corresponding single-phase runs (1–1 and 2–1); the void fraction is the same in the two initial layers, equal to 1.9% in both runs. In the last two bubbly flows (2–3 and 2–4), an initial void fraction difference across the mixing layer is added to the difference in velocity. This results in a rather specific development of the flow as discussed in the following section.

In bubbly flow, the analysis of the bubble size histogram shows that the bubbles consist in a polydispersion of sizes centred on 2 mm but extending up to 4 mm (figure 2). The measured mean and RMS sizes of the bubbles (d_B and d'_B) were estimated as the mean and RMS chord captured by the optical probe. They do not evolve significantly all across the flows (figure 3). So, it can be inferred that either break-up and coalescence do not occur in the flows, or they are in mutual

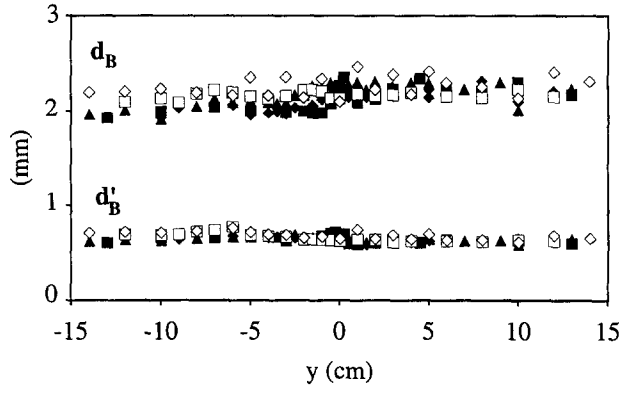

Figure 3. Bubble sizes for run 2–2. x: ■, 6 cm; ◆, 20 cm; ▲, 30 cm; □, 40 cm; ◇, 50 cm.

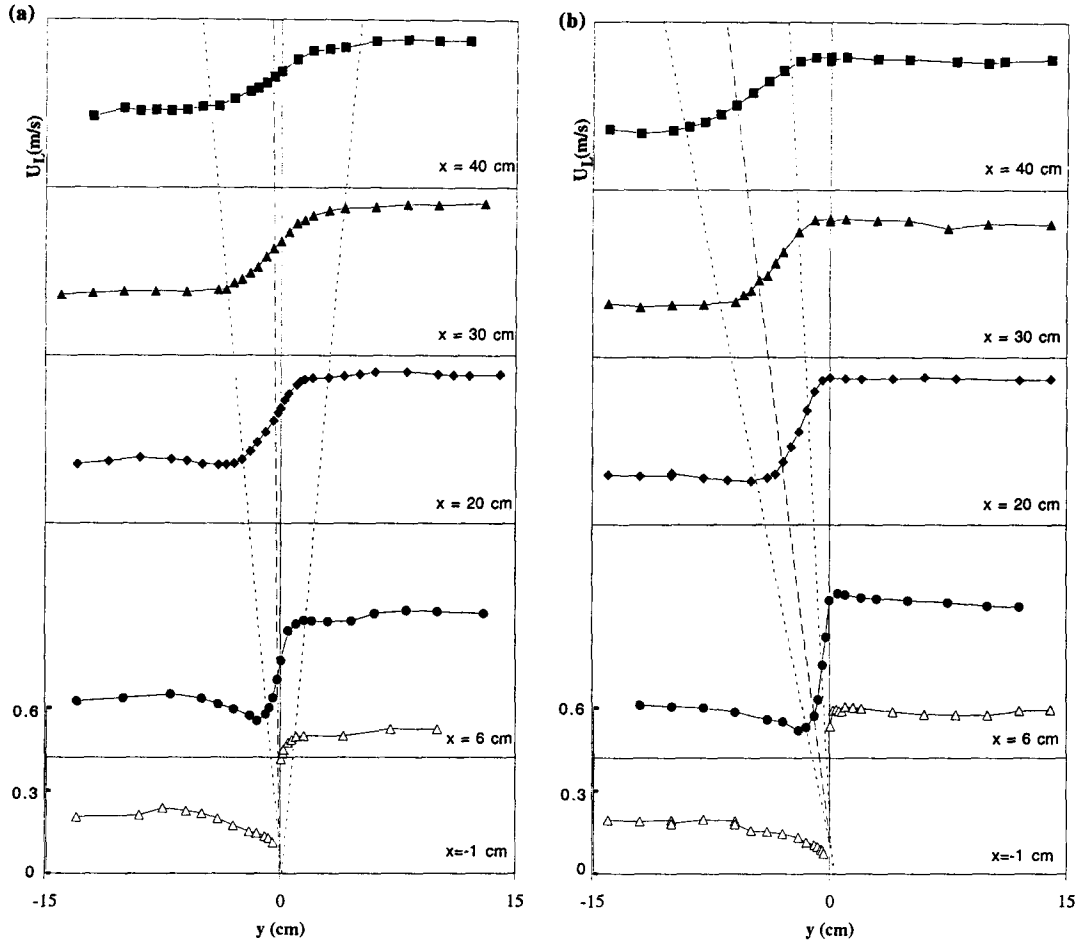

Figure 4. (a) Field of the mean velocity of the liquid phase in bubbly run 2–2. - - - Frontiers of the mixing layer; – – – location of the mean velocity U_{Lm}. (b) Field of the mean velocity of the liquid phase in bubbly run 2–4. - - - Frontiers of the mixing layer; – – – location of the mean velocity U_{Lm}.

equilibrium. Visual observations seem to assess that they do not take place in the mixing layer. Finally, the Reynolds number of the relative movement has a mean value equal to 700.

In this paper, we limit the presentation of the complete results to the results obtained in runs 2–1, 2–2 and 2–4. References to the other runs will be used for general comments or global comparison.

5. MAIN CHARACTERISTICS OF THE FLOWS

The global behaviour of the bubbly flows proved to be very sensitive to void fraction contrasts. The structure of the mean flow may be quite different, depending on the inlet conditions of the void fraction.

When the void fraction of each freestream is the same, the mixing layer is characterised by a development aligned with the splitter plate, and the freestream velocities are conserved downstream (see figure 4(a) for run 2–2).

For the bubbly mixing layers with an initial void fraction difference (2–3, 2–4), the mixing layer bends towards the bubbly freestream. It induces a transverse liquid rate from single-phase to two-phase side. The single-phase freestream is thus decelerated, while the bubbly freestream is accelerated (for run 2–4 see figure 4(b)). The bending is related to the density contrast of the mixtures on both sides of the mixing layer and to subsequent buoyancy effects in a confined geometry.

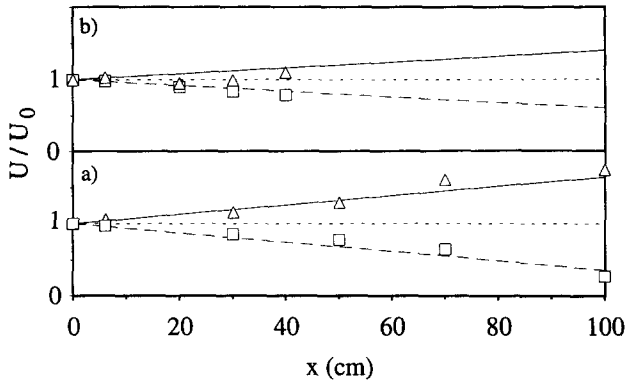

Figure 5. Longitudinal evolution of the mean velocities of the liquid phase in the freestreams: $U_1(x)/U_{10}$ and $U_2(x)/U_{20}$. (a) Run 2–3; (b) run 2–4. Experimental results: □, single-phase side; △, bubble side; [1–2]: – – – single-phase side; — bubbly side.

This phenomenon can be explained if one considers the stationary inviscid problem of the vertical development in a channel of width $2H$ of two immiscible layers of different densities ρ_1 and ρ_2 and inlet velocities U_{10} and U_{20}. For fluids of nearly equal density, an approximate solution of this problem can be found, introducing the small parameter $\epsilon = (\rho_1 - \rho_2)/(\rho_1 + \rho_2)$. The difference in density results in a longitudinal evolution of the freestream velocities U_1 and U_2 and in an inclination of the immiscible boundary located at y_S according to the following expressions:

$$\frac{U_1(x)}{U_{10}} = 1 - \frac{2g\epsilon x}{U_{10}^2 + U_{20}^2}, \qquad [1]$$

$$\frac{U_2(x)}{U_{20}} = 1 + \frac{2g\epsilon x}{U_{10}^2 + U_{20}^2}, \qquad [2]$$

$$\frac{y_S(x)}{2H} = -\frac{g\epsilon x}{U_{10}^2 + U_{20}^2}, \qquad [3]$$

where g is the acceleration due to gravity.

In bubbly flow, estimating ρ_1, ρ_2, respectively as $\rho_1 = (1 - \varepsilon_1)\rho_L$, $\rho_2 = (1 - \varepsilon_2)\rho_L$, a comparison between experimental results and [1], [2] can be made (figure 5). Freestream velocities are correctly estimated from this simple analysis. The location $y_{L1/2}$ of the point where the measured velocity is equal to U_{Lm} characterises the transverse displacement of the mixing layer. Thus, its behaviour can be compared with the evolution of the immiscible boundary. The displacement of $y_{L1/2}$ is small in runs without void fraction contrast, and in runs 2–3 and 2–4 this parameter always evolves from $y = 0$ to the bubbly side of the flow (figure 6). This behaviour is consistent with the effects of the

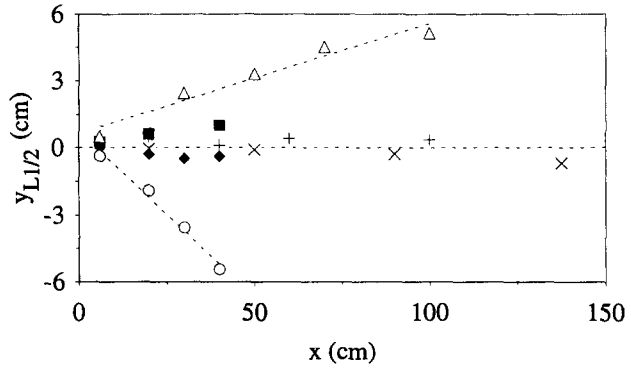

Figure 6. Longitudinal evolution of $y_{L1/2}$. Single-phase runs: +, 1–1; ×, 2–1; bubbly runs: ■, 1–2; ◆, 2–2; △, 2–3; ○, 2–4.

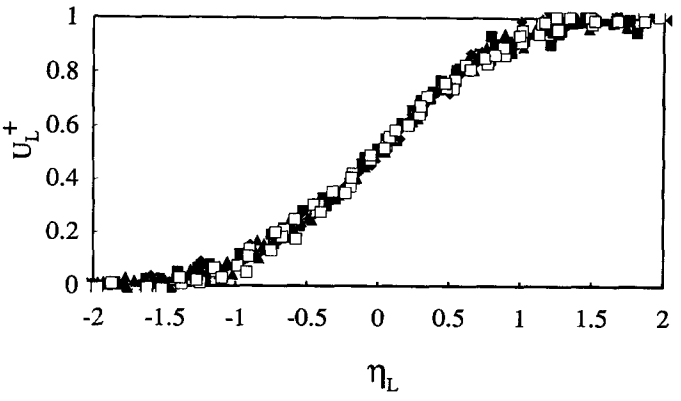

Figure 7. Mean velocity in the liquid phase. Single-phase mixing layer in white: □, run 2–1, 20 cm < x < 138 cm. Bubbly mixing layers in black: ■, run 2–2, 20 cm < x < 50 cm; ▲, run 2–3, 30 cm < x < 100 cm; ◆, run 2–4, 20 cm < x < 40 cm. Goertler's law: —.

contrast of void fraction on both sides of the mixing layer and with the subsequent inclination of the mean flow as described in [3]. The inviscid model predicts accurately the global behaviour of the mean flow.

Moreover, strong instabilities of the interface between bubbly and single-phase flow were observed in run 2–3 (weaker instabilities were also observed in run 2–4). It reveals the strong sensitivity of the mixing layer to a void fraction difference.

6. MEAN VELOCITY FIELDS

For single-phase flows, the evolution of the mean velocity profiles were measured up to a section located at x = 138 cm from the inlet. At a distance of about 20 cm from the inlet, the effects of the wake of the splitter plate disappear and a self-preserving flow is obtained for the mean velocity profiles. The single-phase flows present the main features of free mixing layers without any influence of the lateral walls. In two-phase flows, the splitter plate disturbance is no longer present above x = 20 cm. After this transition region, the mean velocity fields in both phases present a self-similar evolution that keeps the main characteristics of a mixing layer.

6.1. *Mean velocity in the liquid phase*

6.1.1. *Self-preserving profiles*. For single-phase and two-phase runs, mean liquid velocity profiles are plotted in the dimensionless form usually adopted in self-similar analysis of single-phase mixing layers (figure 7). We thus define the dimensionless velocity and coordinates U_L^+ and η_L as

$$U_L^+ = \frac{U_L - U_{L2}}{U_{L1} - U_{L2}}, \qquad [4]$$

$$\eta_L = \sigma_L \frac{(y - y_{L1/2})}{x}, \qquad [5]$$

where $y_{L1/2}$ is defined by $U_L(y_{L1/2}) = U_{Lm}$, and σ_L is a parameter of self-similarity to be adjusted with the experimental lateral expansion.

The self-preserving structure of the mean flow implies that $U_L^+ = f(\eta_L)$.

For single-phase runs as well as for bubbly runs, the comparison is in good agreement with the analytic solution proposed by Goertler (see Rajaratnam 1976):

$$f(\eta_L) = \frac{1}{2}\left[1 + \frac{2}{\sqrt{\pi}} \int_0^{\eta_L} \exp(-u^2)\, du\right]. \qquad [6]$$

The values of σ_L were determined from fitting between measurements and Goertler solution. They are reported in table 1.

In the runs where the freestream velocities evolve due to the aforementioned buoyancy effect, the same law is valid provided that the dimensionless velocity U_L^+ is defined using the local values of the freestream velocities at the corresponding test section: $U_{L1}(x)$, $U_{L2}(x)$. The self-similar structure was also observed for the other runs which have been investigated.

6.1.2. *Lateral expansion*.The lateral development of the mixing layer can be characterised by two parameters: the location of $y_{L1/2}$, and the width of the shear layer B_L.

If $y_{L1/2}$ characterises the bending of the mixing layer, it also gives an indication about the location of the maximum of the velocity gradient. The displacement parameter $y_{L1/2}$ evolves rather linearly with x in every case (figure 6) and its sensitivity to void fraction contrast has been discussed in section 5.

The parameter B_L is typically a length scale of the turbulent diffusion. The width B_L of the mixing layer is defined in a lot of experimental works, as in Liepmann and Laufer (1947), by

$$B_L = | y(U_{L1} - 0.05\Delta U_L) - y(U_{L2} + 0.1\Delta U_L) |. \quad [7]$$

Downstream of the measuring section located at $x = 20$ cm, this parameter varies linearly with x in single-phase flow as well as in bubbly flow (figure 8); thus, the expansions of the mixing layers can be characterised by constant spreading rates dB_L/dx. For the single-phase mixing layers, in the range of velocity ratios explored, the values of the spreading rate are in agreement with those measured by other authors (e.g. Jones *et al.* 1973; Brown and Roshko 1974; Dziomba and Fiedler 1985).

In bubbly mixing layers the transverse expansion is also linear, but the spreading rate is significantly increased. As expected, it appears sensitive to the velocity ratio λ in both single-phase and two-phase flow. But for equal λ, the spreading rate in bubbly flow was found to be more than twice that in the equivalent single-phase flow (table 1). The results for equal λ (runs 1–1 and 1–2 or runs 2–1 and 2–2) testify to such a behaviour. As a consequence, the expansion parameter σ_L is significantly smaller in bubbly flow. For bubbly runs with a void fraction difference between the freestreams, the velocity ratio λ changes downstream but a constant value of the spreading rate still larger than in single-phase runs can be found.

The increase of the spreading rate observed in bubbly mixing layers must be explained.

At first, studies of single-phase mixing layers have shown that the inlet conditions may modify the development of the flow. As shown by Ho and Huang (1982), a subharmonic perturbation of the right frequency of an unforced mixing layer can lead to a strong initial increase of the spreading rate, but the asymptotic spreading rate remains the same. Hussain and Zedan (1978a, 1978b) have shown that in an axisymetric free shear layer, a modification of the initial momentum thickness of the turbulent boundary layer on the splitter plate has negligible effects on the spreading rate. They have also shown that, when the initial fluctuating level of the turbulent boundary layer on the splitter plate is increased, the spreading rate increases. Nevertheless, those inlet effects cannot explain the difference in spreading rates which was observed between single and two-phase mixing

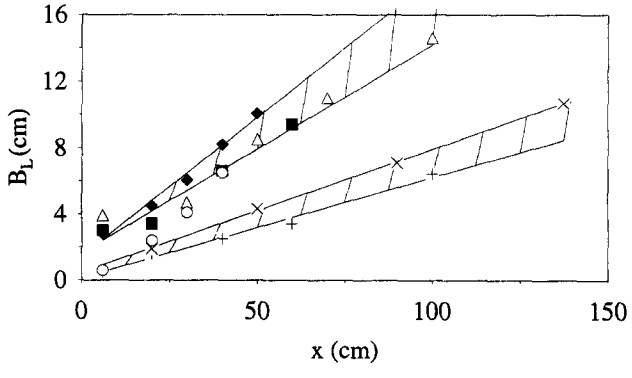

Figure 8. Widths of the mixing layers (see legend of figure 6).

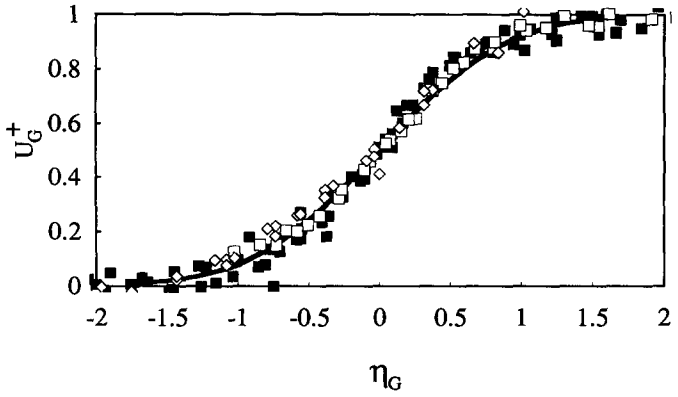

Figure 9. Mean velocity of the bubbles. ■, Run 2–2, 6 cm < x < 50 cm; □, run 2–3, 30 cm < x < 70 cm; ◇, run 2–4, 6 cm < x < 40 cm. Goertler's law: —.

layers, even if bubbles interacting with the upstream boundary layers modify the inlet conditions. In fact, it is not relevant to apply at the present moment the results of Ho and Huang to bubbly mixing layer. Bubble-induced perturbations at first are not periodic. Moreover, even if the mean frequency of the bubbles passages could act as a subharmonic of the right frequency, this subharmonic perturbation could not explain the modification of the asymptotic spreading rate which was achieved in bubbly mixing layers. We have also examined the effect of the enlargement of the momentum thickness θ_0 of the bubbly boundary layers at the end of the splitter plate. This momentum thickness was estimated from the boundary layer on the high velocity side. Its enlargement is unable to explain the differences. The momentum thickness of the mixing layer normalised by θ_0, when examined vs the normalised coordinate x/θ_0, always presents quite the same differences of slopes between single and two-phase runs. Concerning initial fluctuating levels, their influence does not determine the spreading rate modification since, in runs 1–1 and 1–2, they are quite similar while the spreading rate is strongly modified between those runs.

In bubbly flow, the modification of the diffusive length scale development $B_L(x)$ may result from a modification of the shear stress. One could assess that the increase in velocity fluctuations of the liquid due to bubble passages could enhance the shear stress. In order to find agreement with experimental data, the shear stress would have to be greatly enhanced in the absence of interfacial momentum effects. However, preliminary measurement of the shear stress was made in the present study, and the increase in shear stress was minor, in agreement with previous measurements in two-phase flow (Lance *et al.* 1996), with potential theoretical analysis made by Biesheuvel and Van Wijngaarden (1984), or with existing models as developed by Sato and Sekoguchi (1975).

On another side, the dynamic of bubbles in a mixing layer vortex is complex. It induces fluctuations of the relative movement. Liquid is entrained by the bubbles, resulting in added mass forces. It thus seems reasonable to think that bubbles propagate the liquid velocity fluctuations through the mixing layer frontier, and that this mechanism is responsible for the increase in spreading rate.

Thus, interfacial momentum transfer should contribute to the more important spreading rate of the bubbly mixing layers. Effects resulting from the interfacial momentum transfers, and among them specially mean added mass force and its turbulent contribution, are expected to be significant in bubbly mixing layers, and to produce changes in the total spreading rate by means of a supplementary extraction of energy from the mean motion.

6.2. *Mean velocity of the bubbles*

For all bubbly runs, we observed no significant longitudinal or transverse evolution of the slip velocity. The slip velocities are about 30 cm/s. The lower and upper bound of the relative velocity are equal to 27 and 35 cm/s.

The non-dimensional profiles of the bubble velocity show good agreement with the self-preserving profile obtained in liquid phase (figure 9). This is not surprising since the slip velocity is rather constant.

Defining, as in the liquid phase, a width B_G and the location $y_{G1/2}$ it appears that they evolve linearly with x, and stay close to their counterpart values in the liquid phase. The value of the parameter σ_G is of the same order as σ_L (table 1). Thus, it appears that the bubble longitudinal mean motion is primarily controlled by the mean transport by the liquid phase, and an equilibrium between drag and buoyancy forces.

7. VOID FRACTION DISTRIBUTION

The void fraction profiles are plotted in figures 10(a) and 10(b) for two bubbly flows (runs 2–2 and 2–4). For all runs a peak of void fraction exists at the entrance of the flow. The appearance and intensity of this maximum was found to be closely related to the various inlet flow conditions. The development of the bubbly boundary layers over the splitter plate depends on the inlet conditions and is responsible for the formation of the peaks of void fraction. The various appearances of the peaks are in agreement with the experimental observations of Moursali *et al.* (1995) in a bubbly boundary layer over a vertical flat plate.

The void fraction peak decreases in intensity in the flow, even disappears at the last measuring sections, and is displaced significantly in the lateral direction.

The decrease of the peak results from the diffusive effects of small-scale turbulence.

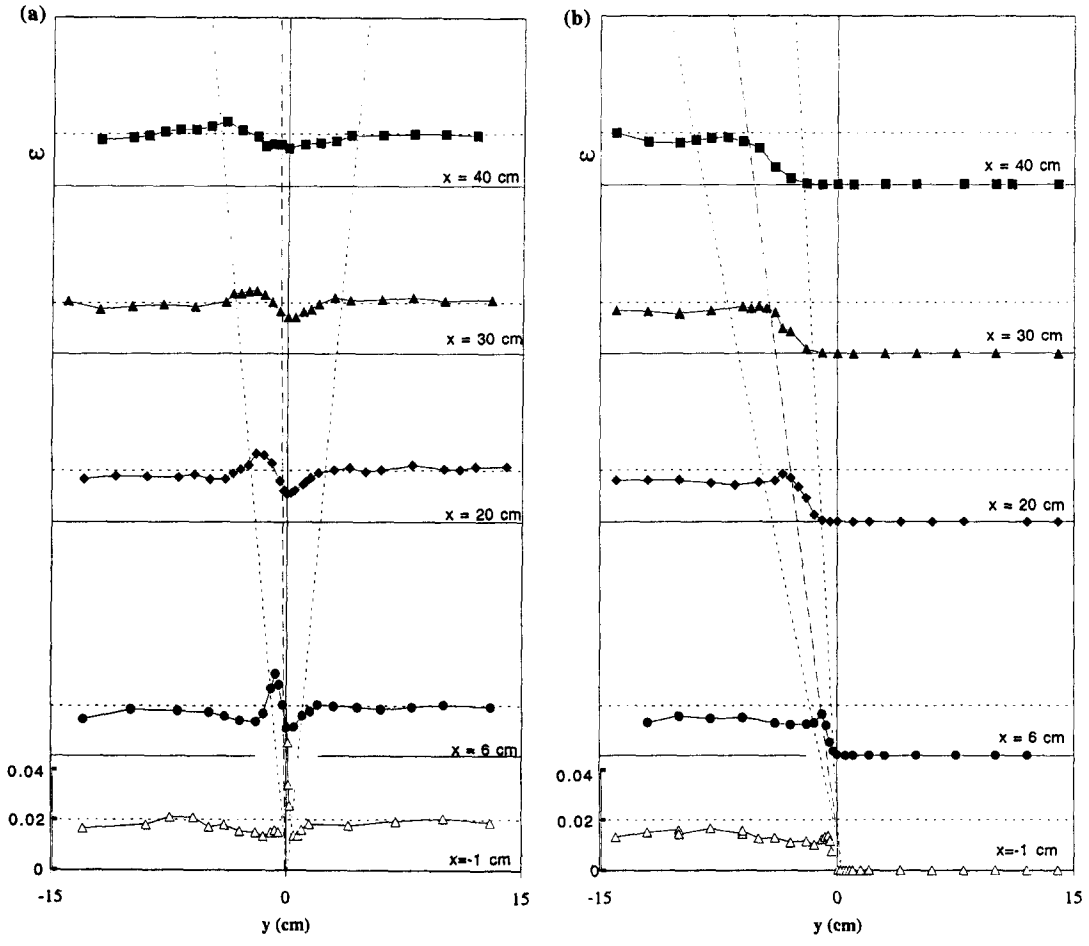

Figure 10. (a) Field of void fraction in bubble run 2–2. - - - Frontiers of the mixing layer; – – – location of the mean velocity U_{Lm}. (b) Field of void fraction in bubbly run 2–4. - - - Frontiers of the mixing layer; – – – location of the mean velocity U_{Lm}.

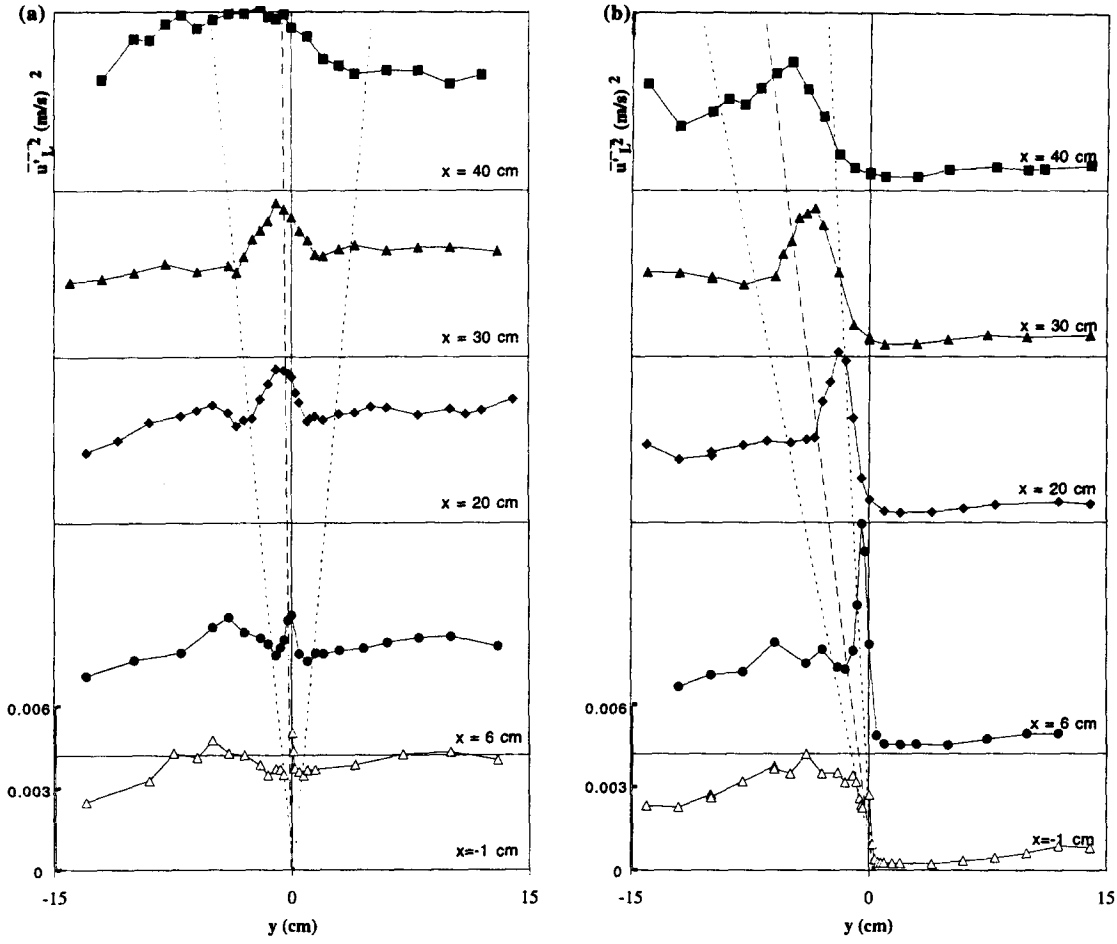

Figure 11. (a) Field of the fluctuating kinetic energy of the liquid phase in bubbly run 2–2. - - - Frontiers of the mixing layer; – – – location of the mean velocity U_{Lm}. (b) Field of the fluctuating kinetic energy of the liquid phase in bubbly run 2–4. - - - Frontiers of the mixing layer; – – – location of the mean velocity U_{Lm}.

The displacement of the peak of void fraction is sensitive to the transverse convection by the liquid phase. In fact, the mean transverse velocity of the liquid induced by the void fraction contrast at the inlet in run 2–4 enhances the lateral migration of the bubbles when compared to the migration in run 2–2. Whatever, the displacement of the peak of void fraction is not identical with the displacement of the mixing layer which follows $y_{L1/2}$. In fact, due to inertia and lift forces, bubbles always undergo a supplementary lateral drift velocity so that their behaviour deviates from scalar diffusion. It is then impossible to obtain a perfect self-similarity of the void fraction profiles as in the downflow mixing layer explored by Sene (1984) where the drift effects were negligible. Sene *et al.* (1994) proved that lift and inertial forces exerted on bubbles in coherent structures can lead bubbles to concentrate on the downflow side of the vortices. This effect can explain the peak displacement toward the low velocity side observed in run 2–2, where the transverse convection is not very important. The evolution of the void fraction profiles in run 2–3 (not presented here) clearly shows that there is a competition between lateral convection and combined effects of lift and inertia forces in the vortices. In the absence of transverse displacement of the mixing layer, these forces would provide a global displacement toward the low velocity side which is not observed. The global transverse displacement of the void fraction is, in this run 2–3, dominated by liquid convection toward the high velocity side.

8. TURBULENCE IN THE LIQUID PHASE

For bubbly runs 2–2 and 2–4, the longitudinal velocity fluctuations of the liquid phase are displayed in figures 11(a) and 11(b). The profiles show that there is a production of fluctuating kinetic energy by the mean shear in the shear layer. On another side, the presence of a low void fraction greatly enhances the fluctuating velocity level all across the bubbly parts of the flows. For run 2–4, in the mixing zone the maximum of turbulence evolves downstream, owing to the accelerations of the freestreams. In the bubbly freestreams, the turbulence levels which are mainly controlled by bubble-induced turbulence in general do not evolve significantly. In run 2–2, above $x = 30$ cm, an increase of the liquid velocity fluctuations appears. This effect, sensitive for the velocity fluctuations, may be related to the tilt of the mixing layer to the low velocity side and to consecutive three-dimensional interactions with the wall. Thus we will only consider the results obtained in the first sections of this case.

8.1. *Dimensionless analysis of the total fluctuating velocity*

The variance of the longitudinal fluctuations of the liquid velocity is plotted in the dimensionless form

$$\overline{u_L'^2}^+ = \frac{\overline{u_L'^2}}{\Delta U_L^2} = h(\eta_L), \qquad [8]$$

where η_L is defined by [5].

In single-phase mixing layer, the results obtained by HFA or by LDA are similar. In the single-phase mixing layer, a real self-similarity of longitudinal fluctuations is achieved above $x = 20$ cm (figure 12). The profiles show a self-preserving form, which is compared with Wygnanski and Fiedler's (1970) data obtained in an air mixing layer. The comparison is not entirely satisfactory: outside the shear layer the levels of fluctuations are higher, in the self-similar region the peak of the streamwise turbulent intensity is slightly greater. Hussain and Zedan (1978a, 1978b) have shown that the maximum of turbulence intensity in a single-phase mixing layer varies with the inlet turbulent levels. While in the experiments of Wygnanski and Fiedler the inlet turbulence levels were negligible, in our experimental facility the flows are turbulent at the entrance. A probable explanation of the differences should thus be found in this inlet feeder memory effect.

In bubbly flows, the dimensionless profiles are plotted for both runs for different locations between 6 and 40 cm (figures 13(a) and 13(b)). For the two bubbly runs, the fluctuating velocity profiles are still self-similar but with a global higher level of turbulence. This gives evidence of the significant contribution of bubble-induced velocity fluctuations, which may cause the maximum of RMS velocity to be displaced from $\eta_L = 0$ (see run 2–2 for example). For run 2–4 the maximum of turbulence in the mixing layer does not evolve significantly when normalized by local $\Delta U_L(x)$, that is when taking into account the accelerations of the freestreams.

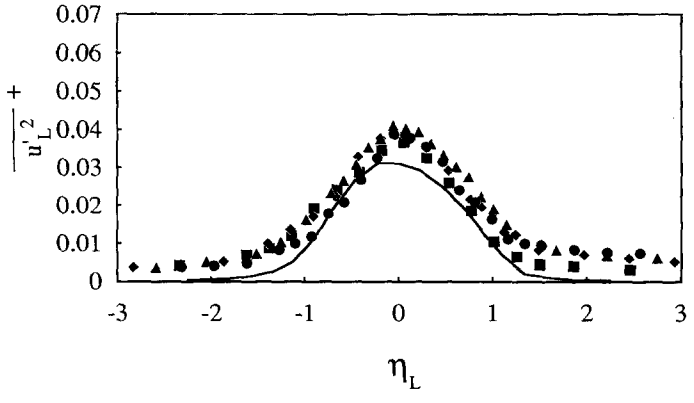

Figure 12. Dimensionless fluctuating kinetic energy in the liquid phase. Single-phase run 2–1. x: ■, 20 cm; ◆, 50 cm; ▲, 90 cm; ●, 138 cm. Wygnanski and Fiedler: —.

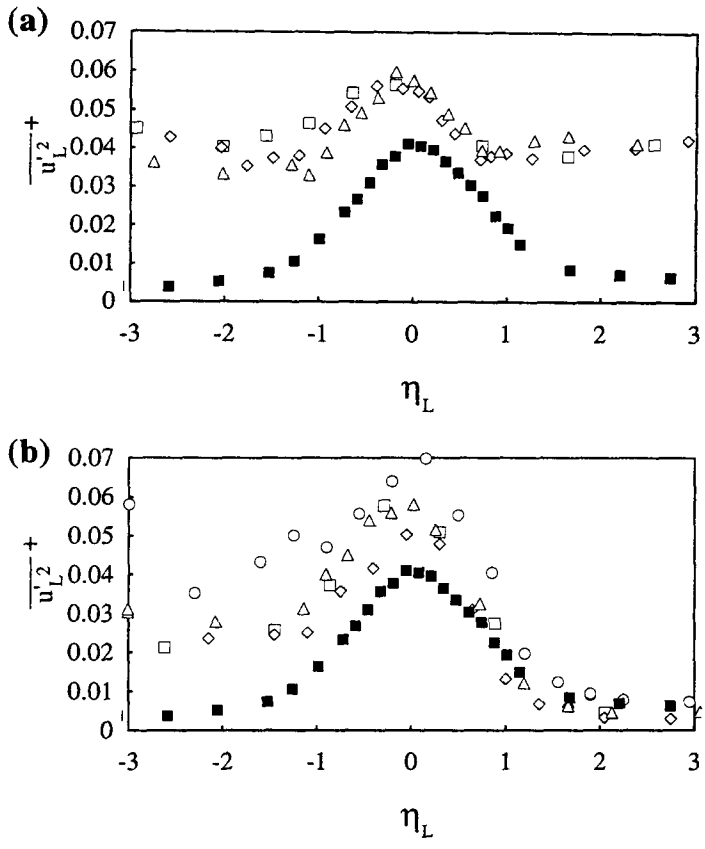

Figure 13. (a) Dimensionless fluctuating kinetic energy in the liquid phase. Bubbly run 2–2. x: □, 6 cm; ◇, 20 cm; △, 30 cm. ■, Single-phase run 2–1. (b) Dimensionless fluctuating kinetic energy in the liquid phase. Bubbly run 2–4. x: □, 6 cm; ◇, 20 cm; △, 30 cm; ○, 40 cm. ■, Single-phase run 2–1.

The non-dimensional analysis based on the scaling of the velocity fluctuations by ΔU_L brings the self-similar superposition of the shear-induced RMS velocity profiles, but it proves to be insufficient to analyse the total "turbulence" structure of the bubbly mixing layers. In bubbly flows there are several velocity and length scales (ΔU_L, $U_G - U_L$, $B_L(x)$, d_B, mean spacing between bubbles). In our experimental conditions, ΔU_L and $U_G - U_L$ have the same order of magnitude. Thus, bubble-induced turbulence is relatively more important than in bubbly experiments at higher velocity (Sun and Faeth 1986; Bel Fdhila *et al.* 1990). Obviously, turbulence models with only one set of velocity and length scales should be unable to work well in our bubbly flows. It is thus clear that it is necessary to separate each contribution to the liquid velocity fluctuations produced either by the mean shear stress or by the slip velocity in order to clarify the nature of "turbulence" in bubbly flows.

8.2. *An attempt to separate bubble-induced and shear-induced components*

An attempt to separate bubble-induced and shear-induced components was tried. It consists in an approximate separation using a heuristic model which is based on the experimental results obtained by Lance and Bataille (1991) in a uniform bubbly flow. The purpose is to discuss the conceptual idea of adding uncorrelated fluctuating kinetic energy produced either by the mean shear stress or by the bubble passages in order to rebuild the total kinetic energy in the case of a mixing layer. Such a decomposition is, of course, not rigorous as it does not consider nonlinear coupling between the random motions induced by the bubbles and the random field of shear-induced fluctuations. However, it allows discussion of recent turbulence models for bubbly flows at low void fraction. In those models, the two parts of the fluctuating kinetic energy, obeying different production mechanisms, are governed by distinct transport equations (Lopez de Bertodano *et al.* 1994a, 1994b).

Thus, we want to analyse the possibility of writing the total longitudinal fluctuating energy measured in the liquid phase $\overline{u_L'^2}$ as the sum of the longitudinal fluctuating energy which is induced by the bubbles $\overline{u_{BI}'^2}$, and of the longitudinal fluctuating energy induced by the mean shear stress in the bubbly flow $\overline{u_{SI}'^2}$:

$$\overline{u_L'^2} = \overline{u_{SI}'^2} + \overline{u_{BI}'^2}. \quad [9]$$

It must be noted that the shear stress is modified by bubble presence from the shear stress in single-phase flow with identical phasic velocity of the liquid at the inlet. In fact, for identical inlet conditions, the bubbly and single-phase mixing layers expand differently. It is thus not possible to identify shear-induced turbulence distributions in the single and two-phase flows. Therefore, we will examine the residual fluctuating kinetic energy $\overline{u_R'^2}$ obtained after subtraction of a modelled bubble-induced contribution from the total measured fluctuating kinetic energy. We will compare the residual fluctuating kinetic energy with a purely shear-induced type one, without treating the problem of prediction of the shear-induced component in bubbly flow.

A representative expression of the bubble-induced fluctuating kinetic energy in bubbly flow can be identified from experimental and theoretical results. Bubble-induced fluctuating kinetic energy has been calculated by Van Wijngaarden (1976) or Biesheuvel and Van Wijngaarden (1984) for spherical bubbles in a potential flow. On the other hand, Lance and Bataille (1991) calculated the bubble-induced longitudinal fluctuating kinetic energy in a potential flow for spheroidal bubbles experiencing helicoidal trajectories. In both studies, bubble-induced turbulence resulted from added mass effects, and was proportional to the void fraction times the square of the slip velocity. Whatever, due to rectilinear path, or helicoidal trajectory, the amount of fluctuating kinetic energy was quite different. Lance and Bataille also measured longitudinal fluctuating kinetic energy $\overline{u_{BI}'^2}$ generated by air bubbles rising in stagnant water. They found good agreement between their measurements and calculus. The kinetic energy was

$$\overline{u_{BI}'^2} \approx \epsilon(U_G - U_L)^2. \quad [10]$$

Moreover, in the bubbly grid-generated turbulent flow, Lance and Bataille (1991) showed that, for low enough values of the void fraction, the turbulent energy excess associated with the bubble contribution can be written as in [10]. This result was independent of the velocity fluctuation level generated by the grid, showing that [9] can hold in low void fraction bubbly flow. The turbulent energy excess did not evolve with the distance from the grid. As noted by Lance and Bataille, the bubble-induced turbulence is related to the power developed by added mass force in the relative movement, and fluctuations in the wakes should not contribute much to fluctuating kinetic energy. Wake contributions consist essentially in a strong modification of the viscous dissipation rate, which scales with the drag power. These results have been confirmed in the bubbly mixing layer by recent spectral measurements (Roig *et al.* 1995).

Thus we take [10] as a model for $\overline{u_{BI}'^2}$ as resulting from added mass effects.

In figures 14(a) and 14(b), for the two bubbly mixing layers, we have reported in non-dimensional coordinates the residual fluctuating kinetic energy of the liquid phase $\overline{u_R'^2}$ obtained after subtraction of $\overline{u_{BI}'^2}$ from the total measured one $\overline{u_L'^2}$.

In case 2–4 the residual fluctuating kinetic energy is of shear-induced type. Its behaviour is then consistent with the splitting of fluctuating kinetic energy into two contributions rather statistically independent.

Less typical results are obtained for cases 2–2 and 2–3, where this crude approximation of the bubble-induced turbulence is not quite satisfactory. Uncertainties in the slip velocity measurements can explain a part of the residual scattering. But the idea of splitting the kinetic energy into two parts seems reasonable. Whatever, the model for $\overline{u_{BI}'^2}$ is primarily too simple. At first, it neglects a non-turbulent local effect of mutual hydrodynamic interactions between bubbles which should increase with the void fraction. Then, it is based on added mass effects in helicoidal trajectories of the bubbles and does not take into account the added mass effects in large scale fluctuations of the liquid which are presumed to be important in mixing layers.

Nevertheless, the promising results obtained for run 2–4 suggest that, at low void fraction, for a global turbulence prediction, one can think about separation of bubble-induced and shear-induced components of the fluctuating kinetic energy, even in an inhomogeneous shear flow

like the mixing layer. Following Lopez de Bertodano *et al.* (1994), shear-induced turbulence modelling could be derived from the standard single-phase modelling, eventually including eddy viscosity modification by bubbles. But on the other hand, bubble-induced turbulence modelling should take into account the local dynamic of pseudo-turbulence, through a pseudo-turbulence transport equation including as source term the local power of the added mass instead of a modelled mean effect of the added mass (Lopez de Bertodano *et al.* 1994).

9. BUBBLE VELOCITY FLUCTUATIONS

The ratio of the RMS velocity in gas phase to the RMS velocity in liquid phase (C_t) is an important parameter for numerical computations in the two-fluid model formulation. Usually, the ratio C_t is related to the dispersion of the bubbles by the turbulence of the continuous phase.

In figure 15 the experimental results obtained in bubbly run 2–2 are displayed. The value of C_t is found nearly constant with a mean value $C_t = 1.5$. There is no evolution of C_t in the flow. The results are similar for the other bubbly runs, and within data scatter C_t is between 1.1 and 1.8.

Tchen's theory for dispersion predicts a value of C_t depending on the bubble relaxation time and on the integral time scale of turbulence for bubbles whose diameter is larger than the Kolmogorov length scale (Hinze 1959). In the bubbly mixing layer, the integral length scale is of the same order of magnitude as the width B_L, and so evolves downstream (Roig *et al.* 1995). The integral time scale thus also evolves downstream, while the temporal scale characteristic of the bubble entrainment does not vary. So, according to the present theory of dispersion, C_t should vary with x. The prediction from Tchen's theory leads to decreasing values of C_t between section $x = 6$ cm and section $x = 50$ cm, in the range of experimental results. Even if the order of magnitude of

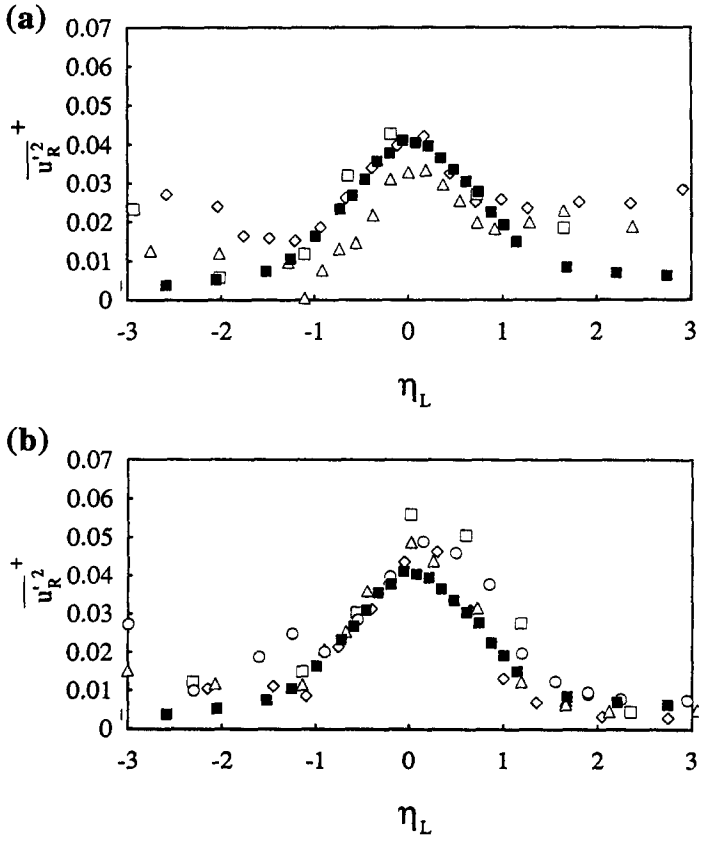

Figure 14. (a) Residual fluctuating kinetic energy in the liquid phase: $\overline{u_R'^2}^+ = \overline{u_L'^2}^+ - \overline{u_{BI}'^2}^+$. Bubbly run 2–2: x: □, 6 cm; ◇, 20 cm; △, 30 cm. ■, Single-phase run 2–1. (b) Residual fluctuating kinetic energy in the liquid phase: $\overline{u_R'^2}^+ = \overline{u_L'^2}^+ - \overline{u_{BI}'^2}^+$. Bubbly run 2–4: x: □, 6 cm; ◇, 20 cm; △, 30 cm; ○, 40 cm. ■, Single-phase run 2–1.

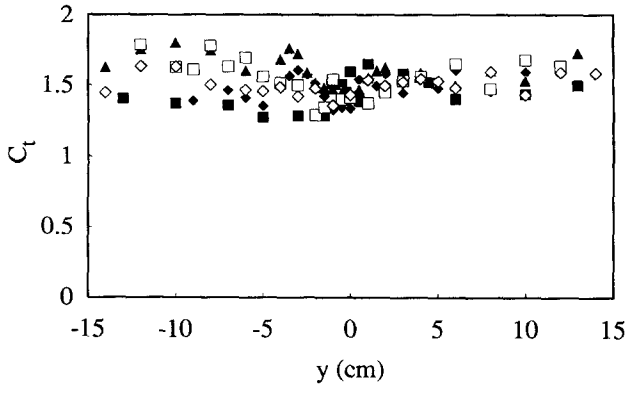

Figure 15. Ratio of the velocity fluctuations in both phases for bubbly run 2–2. x: ■, 6 cm; ◆, 20 cm; ▲, 30 cm; □, 40 cm; ◇, 50 cm.

the experimental data is close to the theoretical prediction, in our flow conditions the modelling of the dispersed phase stress tensor is not a matter of purely turbulent dispersion. The slip velocity is comparable to the velocity difference across the mixing layer. Thus, bubbles respond to the spectrum of all the velocity fluctuations of the liquid phase largely modified by the "pseudo-turbulence". Moreover, the fluctuating motion of the bubbles is not entirely controlled by the dispersion due to large scale motions of the fluid: an important contribution to the fluctuations of the velocity of the bubbles is due to their helicoidal trajectories self-induced by their wakes, and not to turbulent dispersion.

10. CONCLUSIONS

Local investigation has been achieved in turbulent bubbly mixing layers. New experimental results were obtained in flow cases where the velocity fluctuations of the liquid induced by the bubbles were of the same order of magnitude as the turbulence induced by the shear stress. Void fraction, mean velocities and turbulent fluctuations in the liquid phase are provided. For various flow conditions, these measurements are completed by the measurements of velocity and size of the bubbles. The physical analysis of the present results shows the main characteristics of this bubbly flow.

—The general behaviour of the flow proves to be very sensitive to the void fraction contrast at the inlet section. In fact, even low void fraction contrast can induce a strong acceleration of the bubbly side of the mixing layer, and a bending of the flow. Due to this, it was observed that plane mixing layers were difficult to obtain.

—The presence of a peak of void fraction created by the splitter plate is observed. This peak decreases in intensity and is displaced significantly in the lateral direction owing to the forces experienced by the bubbles and to the transverse displacement of the mixing layer.

—The mean velocity presents a similar self-preserving evolution in both phases. The slip velocity is found rather constant owing to an equilibrium between drag and buoyancy. The self-similar behaviour of the mean velocity in bubbly mixing layer is formally identical to the self-similar behaviour of single-phase mixing layer. Nevertheless the lateral expansion in bubbly flow is more important than in single-phase flow. This enlargement of the spreading rate was analysed as an effect of a supplementary liquid entrainment due to the added mass of the bubbles.

—In our flow conditions, the velocity fluctuations in the liquid phase are strongly modified from their single-phase values. The main result concerns an important amount of velocity fluctuation in liquid phase, essentially controlled by the relative velocity of the bubbles. Fluctuating kinetic energy in bubbly flow is found to result approximately from the superposition of shear-induced type contribution and bubble-induced contribution identified as a local non-turbulent effect of added mass force.

—The ratio C_t between bubble velocity fluctuation and liquid velocity fluctuation is found constant all over the flow, probably due to a large contribution of helicoidal movements.

Finally, in order to improve numerical prediction and turbulence models, these experimental results suggest that it is possible, at least for low void fraction, to distinguish the contribution of the "pseudo-turbulence" directly created by the added mass of the bubbles from the turbulence produced by the shear flow. The analysis of their interaction and coupling, as well as the study of the role of coherent structures in bubble transport, are the next steps towards increasing the completeness of the description of turbulent bubbly mixing layers.

REFERENCES

Bel Fdhila, R. and Simonin, O. (1992) Eulerian prediction of a turbulent bubbly flow downstream of a sudden pipe expansion. Proceedings of the 6th Workshop on Two-phase Flow Predictions, 30 March–2 April, Erlangen.

Bel Fdhila, R., Suzanne, C. and Masbernat, L. (1990) Local measurements in two-phase bubbly flows in complex geometries. *Phase–Interphase Phenomena in Multiphase Flow*, Proceedings of International Seminar of Heat and Mass Transfer, May 1990, Dubrovnik, Yugoslavia. I.C.H.M.T., pp. 245–257.

Biesheuvel, A. and Van Wijngaarden, L. (1984) Two-phase flow equations for a dilute dispersion of gas bubbles in liquid. *J. Fluid Mech.* **148,** 301–318.

Brown, G. and Roshko, A. (1974) On density effects and large structure in turbulent mixing layers. *J. Fluid Mech.* **64,** 775–816.

Cartellier, A. (1990) Optical probes for local void fraction measurements: characterisation of performance. *Rev. Sci. Instrum.* **61,** 874–886.

Drew, D. A. and Lahey, R. T. (1982) Phase distribution mechanisms in turbulent low-quality two-phase flow in a circular pipe. *J. Fluid Mech.* **117,** 91–106.

Drew, D. A. and Wallis, G. B. (1994) Fundamentals of two-phase flow modelling. In *Multiphase Science and Technology*, Vol. 8, *Two-Phase Flow Fundamentals*. Begell House, Wallingford, U.K., pp. 1–68.

Dziomba, B. and Fiedler, H. E. (1985) Effect of initial conditions on two-dimensional free shear layers. *J. Fluid Mech.* **152,** 419–442.

Gherson, P. and Lykoudis, P. S. (1984) Local measurements in two-phase liquid–metal magnetofluid-mechanic flow. *J. Fluid Mech.* **147,** 81–104.

Herringe, R. A. and Davis, M. R. (1976) Structural development of gas–liquid mixture flows. *J. Fluid Mech.* **73,** 97–123.

Hinze, J. O. (1959) *Turbulence. An Introduction to its Mechanism and Theory*. McGraw-Hill, New York.

Ho, C.-M. and Huang, L.-S. (1982) Subharmonics and vortex merging in mixing layers. *J. Fluid Mech.* **119,** 443–473.

Hussain, A. K. M. F. and Zedan, M. F. (1978a) Effects of the initial condition on the axisymmetric free shear layer: effects of the initial momentum thickness. *Phys. Fluids* **21,** 1100–1112.

Hussain, A. K. M. F. and Zedan, M. F. (1978b) Effects of the initial condition on the axisymmetric free shear layer: effect of the initial fluctuation level. *Phys. Fluids* **21,** 1475–1481.

Jones, B. G., Planchon, H. P. and Hammersley, R. J. (1973) Turbulent correlation measurements in a two-stream mixing layer. *AIAA J.* **11,** 1146–1150.

Lance, M. and Bataille, J. (1991) Turbulence in the liquid phase of a uniform bubbly air–water flow. *J. Fluid Mech.* **222,** 95–118.

Lance, M. and Lopez de Bertodano, M. (1994) Phase distribution phenomena and walls effects in bubbly two-phase flows. In *Multiphase Science and Technology*, Vol. 8, *Two-Phase Flow Fundamentals*. Begell House, Wallingford, U.K. pp. 69–124.

Lance, M., Marié, J. L. and Bataille, J. (1991) Homogeneous turbulence in bubbly flows. *J. Fluid. Eng.* **113,** 295–300.

Lance, M., Marié, J. L., Moursali, E., Bataille, J., Suzanne, C., Roig, V., Bel Fdhila, R. and Masbernat, L. (1996) Experimental study of turbulent bubbly shear flows. *Chem. Eng. Commun.* **141–142,** 51–70.

Liepmann, H. W. and Laufer, J. (1947) Investigations of free turbulent mixing. N.A.C.A. Tech. Note No. 1257.

Lopez de Bertodano, M., Lahey, R. T. and Jones, O. C. (1994a) Phase distribution in bubbly two-phase flow in vertical ducts. *Int. J. Multiphase Flow* **20,** 805–818.

Lopez de Bertodano, M., Lahey, R. T. and Jones, O. C. (1994b) Development of a k-e model for bubbly two-phase flow. *J. Fluid. Eng.* **116,** 128–134.

Moursali, E., Marié, J. L. and Bataille, J. (1995). An upward turbulent bubbly layer along a vertical flat plate. *Int. J. Multiphase Flow* **21**(1), 107–117.

Rajaratnam, N. (1976) *Turbulent Jets. Elsevier Science*, Amsterdam.

Roig, V. (1993) Zone de mélange d'écoulements diphasiques à bulles. Ph.D. Thesis, University of Toulouse, France.

Roig, V., Larrieu, N. and Suzanne, C. (1995) Turbulent length scales in a bubbly mixing layer. *Proceedings of the International Symposium on Two-Phase Flow Modelling and Experimentation*, October 9–11, Rome, Vol. 1, pp. 383–388.

Sato, Y. and Sekoguchi, K. (1975) Liquid velocity distribution in two-phase bubble flow. *Int. J. Multiphase Flow* **2,** 79–95.

Sene, K. J. (1984) Aspects of bubbly two-phase flow. Ph.D. Thesis, University of Cambridge, U.K.

Sene, K. J., Hunt, J. C. R. and Thomas, N. D. (1994) The role of coherent structures in bubble transport by turbulent shear flows. *J. Fluid Mech.* **259,** 219–240.

Serizawa, A., Kataoka, I. and Michiyoshi, I. (1975) Turbulence structure of air–water bubbly flow. *Int. J. Multiphase Flow* **2,** 221–259.

Sun, T. Y. and Faeth, G. M. (1986) Structure of turbulent bubbly jets. *Int. J. Multiphase Flow* **12,** 99–126.

Theofanous, T. G. and Sullivan, J. (1982) Turbulence in two-phase dispersed flows. *J. Fluid Mech.* **116,** 343–362.

Van der Welle, R. (1985) Void fraction, bubble velocity and bubble size in two-phase flow. *Int. J. Multiphase Flow* **11,** 317–345.

Van Wijngaarden, L. (1976) Hydrodynamic interaction between gas bubbles in liquid. *J. Fluid Mech.* **77,** 27–44.

Wang, S. K., Lee, S. J., Jones, O. C. and Lahey, R. T. (1987) Three-dimensional turbulence structure and phase distribution measurements in bubbly two-phase flows. *Int. J. Multiphase Flow* **13,** 327–343.

Wang, S. K., Lee, S. J., Jones, O. C. and Lahey, R. T. (1990) Statistical analysis of turbulent two-phase pipe flow. *J. Fluid. Eng.* **112,** 89–95.

Wygnanski, I. and Fielder, H. E. (1970) The two-dimensional mixing region. *J. Fluid Mech.* **41,** 327–361.